



Article

Comparison of the Drug-Induced Efficacies between Omidenepag Isopropyl, an EP2 Agonist and PGF2 α toward TGF- β 2-Modulated Human Trabecular Meshwork (HTM) Cells

Soma Suzuki ¹, Masato Furuhashi ², Yuri Tsugeno ¹, Araya Umetsu ¹, Yosuke Ida ¹, Fumihito Hikage ¹, Hiroshi Ohguro ¹ and Megumi Watanabe ^{1,*}

¹ Departments of Ophthalmology, School of Medicine, Sapporo Medical University, Chuo-ku, Sapporo 060-8556, Japan; ophthalsoma@sapmed.ac.jp (S.S.); yuri.tsugeno@gmail.com (Y.T.); araya.umetsu@sapmed.ac.jp (A.U.); funky.sonic@gmail.com (Y.I.); fuhika@gmail.com (F.H.); ooguro@sapmed.ac.jp (H.O.)

² Departments of Cardiovascular, Renal and Metabolic Medicine, Sapporo Medical University, Sapporo 060-8556, Japan; furuhashi@sapmed.ac.jp

* Correspondence: watanabe@sapmed.ac.jp; Tel.: +81-611-2111

Abstract: To compare the drug-induced efficacies between omidenepag (OMD), an EP2 agonist, and prostaglandin F2 α (PGF2 α) on glaucomatous trabecular meshwork (TM) cells, two- and three-dimensional (2D and 3D) cultures of TGF- β 2-modulated human trabecular meshwork (HTM) cells were used. The following analyses were performed: (1) transendothelial electrical resistance (TEER) and FITC-dextran permeability measurements (2D), (2) the size and stiffness of the 3D spheroids, and (3) the expression (both 2D and 3D) by several extracellular matrix (ECM) molecules including collagen (COL) 1, 4 and 6, and fibronectin (FN), and α smooth muscle actin (α SMA), tight junction (TJ)-related molecules, claudin11 (Cldn11) and ZO1, the tissue inhibitor of metalloproteinase (TIMP) 1–4, matrix metalloproteinase (MMP) 2, 9 and 14, connective tissue growth factor (CTGF), and several endoplasmic reticulum (ER) stress-related factors. TGF- β 2 significantly increased the TEER values and decreased FITC-dextran permeability, respectively, in the 2D HTM monolayers, and induced the formation of downsized and stiffer 3D HTM spheroids. TGF- β 2-induced changes in TEER levels and FITC-dextran permeability were remarkably inhibited by PGF2 α . PGF2 α induced increases in the sizes and stiffness of the TGF- β 2-treated 3D spheroids, but OMD enhanced only spheroid size. Upon exposure to TGF- β 2, the expression of most of the molecules that were evaluated were significantly up-regulated, except some of ER stress-related factors were down-regulated. TJ-related molecules or ER stress-related factors were significantly up-regulated (2D) or down-regulated (3D), and down-regulated (2D) by PGF2 α and OMD, while both drugs altered the expression of some of the other genes in the 3D spheroids in a different manner. The findings presented herein suggest that PGF2 α and OMD differently modulate the permeability of the TGF β 2-modulated 2D monolayers and the physical properties of the 3D HTM spheroids.

Keywords: 3D spheroid cultures; human trabecular meshwork; omidenepag isopropyl; omidenepag; PGF2 α ; TGF β 2



Citation: Suzuki, S.; Furuhashi, M.; Tsugeno, Y.; Umetsu, A.; Ida, Y.; Hikage, F.; Ohguro, H.; Watanabe, M. Comparison of the Drug-Induced Efficacies between Omidenepag Isopropyl, an EP2 Agonist and PGF2 α toward TGF- β 2-Modulated Human Trabecular Meshwork (HTM) Cells. *J. Clin. Med.* **2022**, *11*, 1652. <https://doi.org/10.3390/jcm11061652>

Academic Editors: Anna Maria Bassi and Stefania Vernazza

Received: 20 January 2022

Accepted: 13 March 2022

Published: 16 March 2022

Publisher's Note: MDPI stays neutral with regard to jurisdictional claims in published maps and institutional affiliations.



Copyright: © 2022 by the authors. Licensee MDPI, Basel, Switzerland. This article is an open access article distributed under the terms and conditions of the Creative Commons Attribution (CC BY) license (<https://creativecommons.org/licenses/by/4.0/>).

1. Introduction

In terms of the etiology of glaucoma [1,2], it is well known that elevated levels of the intraocular pressure (IOP) are critical factors [3], and therefore, hypotensive therapies by the use of anti-glaucoma medications in conjugation with laser or surgical intervention is recognized as the only currently available evidence-based therapy [4]. Physiologically, IOP levels of the human eye are maintained by aqueous humor (AH) dynamics, that is, AH production and drainage occur mainly through the trabecular meshwork (TM) pathway [5]. The cause of such an IOP elevation is generally thought to be due to an elevated resistance

to AH drainage through the TM pathway presumably by the excess depositions of several extracellular matrix (ECM) molecules [6]. It has been reported that such an excess of ECM deposits of TM may be mediated by elevated AH levels of transforming growth factor (TGF)- β 2 [7]. In fact, an *in vitro* study using a rat model indicated that TGF- β 2 caused an elevation in IOP levels by increasing the resistance to AH outflow [8]. As a result, TGF- β 2 is now commonly used as an *in vitro* model using the TM cell cultures [9].

In addition to the first-line drugs, prostaglandin (PG) F 2α agonists (PGF 2α -ags) are used in the treatment of patients with glaucoma and ocular hypertension (OH) [10–12], omidenepag isopropyl (OMDI), a non-prostaglandin, a prostanoid EP2 agonist, has recently become available [13,14]. Pharmacologically, (1) OMDI is metabolized into the active form (omidenepag, OMD) by hydrolysis after its administration, and (2) the hypotensive mechanisms for OMD involve an increase in the ease of uveoscleral outflow, similar to PGF 2α -ags [15]. However, a recent *in vivo* study reported that the pharmacokinetics are quite different for OMD compared to PGF 2α -ags [16]. In addition, the effects of these drugs on the ease of conventional outflow have not been extensively characterized at this time, since an appropriate experimental model for evaluating the drug efficacies on conventional versus uveoscleral roots has not been available. To address this difficulty, we recently succeeded in preparing a 3D human TM (HTM) spheroid as a suitable *in vitro* model [17], in which no assistance, such as a collagen-gel or a scaffold that is usually used in the 3D culture method [18], was required.

Therefore, in the current study, to compare the roles between PGF 2α -ags and an EP2 agonist in glaucomatous HTM, we used TGF- β 2-treated 2D and 3D HTM cells and subjected them to the following analyses; (1) the transendothelial electrical resistance (TEER) and FITC-dextran permeability (2D), (2) the physical properties of 3D spheroids, including size and stiffness, and (3) the expression of major extracellular matrix (ECM) molecules including collagen (COL) 1, 4 and 6, fibronectin (FN) and α smooth muscle actin (α SMA), tight junction (TJ) related molecules, claudin11 (Cldn11) and ZO1, tissue inhibitors matrix proteinase (TIMP) 1–4, matrix metalloproteinase (MMP) 2, 9 and 14, and connective tissue growth factor (CTGF), and endoplasmic reticulum (ER) stress-related factors (2D and 3D).

2. Materials and Methods

2.1. Human Trabecular Meshwork (HTM) Cells

All experiments using human-derived cells were conducted in compliance with the tenets of the Declaration of Helsinki after approval by the internal review board of Sapporo Medical University. Immortalized HTM cells transfected with an original defective mutant of the SV40 virus were purchased from Applied Biological Materials Inc., Richmond, Canada, and these cells were characterized as described in the consensus recommendations for TM cells [19] in advance of the current study described below.

2.2. 2D and 3D Spheroid Cultures of Human Trabecular Meshwork (HTM) CELLS

The 2D-cultured HTM cells were further processed to obtain 3D spheroids in a hanging droplet culture plate (# HDP1385, Sigma-Aldrich Co., St. Louis, MO, USA) during a period of 6 days as described in our previous report [17] in the absence or presence of 5 ng/mL TGF- β 2 and/or either 100 nM PGF 2α or Omidenepag (OMD). The dosages of these TGF- β 2 and PG derivatives were identical to those used in our previous studies [17,20,21].

2.3. Transendothelial Electron Resistance (TEER) and FITC Dextran Permeability Measurements of 2D HTM Cultured Monolayer

Barrier functions of the 2D HTM cell monolayers were evaluated by TEER and FITC-dextran permeability measurements, as described previously using 12-well plates for TEER (0.4 μ m pore size and 12 mm diameter; Corning Transwell, Sigma-Aldrich) and the TEER values (Ω cm 2) were recorded by an electrical resistance system (KANTO CHEMICAL Co., Inc., Tokyo, Japan) [17,22]. Concerning FITC-dextran permeability, the concentrations of the

FITC-dextran that penetrated through the 2D monolayer during a period of 60 min were determined using a multimode plate reader (Enspire; Perkin Elmer, MA, USA).

2.4. Physical Properties Measurements, including the Size and Stiffness, of 3D Spheroids

The physical properties, size, and stiffness of the 3D HTM spheroids were evaluated by measurements of the largest cross-sectional area (CSA) from phase-contrast images and the force ($\mu\text{N}/\mu\text{m}$) required to induce a 50% deformation during a 20 s period by a micro-squeezer (MicroSquisher, CellScale, Waterloo, ON, Canada), respectively, as previously reported [17,23].

2.5. Quantitative PCR

Quantitative PCR was performed using the specific primers (Supplemental Table S1A), and fold-changes in the normalized housekeeping gene 36B4 (Rplp0) were calculated as described previously [17]. Primers' information and running protocols were described in Supplemental Table S1B, respectively.

2.6. Immunofluorescent Labeling

Immunofluorescent labeling of 2D- and 3D-cultured HTM was performed by a previously described method. Briefly, after blocking in 3% BSA in PBS, the 4% paraformaldehyde (PFA) fixed 2D-cultured cells or 3D spheroids were successively incubated with (1) a primary antibody (1:200 dilution) including anti-collagen 1, 4 or 6 (#600-401-103-0.1, #600-401-106-0.1, #600-401-108-0.1, ROCKLAND antibodies & assays, Limerick, PA, USA), anti-fibronectin (#sc-8422, Santa Cruz Biotechnology, INC. Dallas, TX, USA) or anti- α SMA (#ab5694, Abcam, Cambridge UK) details of these primary antibodies are listed in Supplemental Table S2), and (2) an Alexa Fluor 488 labeled secondary antibody (1:500 dilution), and phalloidin (#A12379, ThermoFisher, Waltham, MA, USA) and DAPI (1:1000 dilution) (#D523, Doujin, Japan). Their immunofluorescent images were obtained using a Nikon A1 confocal microscope and NIS-Elements 4.0 software as described previously [17].

2.7. Statistical Analysis

All statistical analyses were performed using Graph Pad Prism 9 (GraphPad Software, San Diego, CA, USA), and statistical significance was determined by a confidence level greater than 95% in a two-tailed Student's *t*-test or two-way analysis of variance (ANOVA) followed by a Tukey's multiple comparison test was performed as described previously [17].

3. Results

To compare the effect of $\text{PGF2}\alpha$ and an EP2 agonist, omidenepag (OMD), on glaucomatous human TM, 2D- and 3D-cultured HTM cells that had been treated with $\text{TGF-}\beta$ 2 (5 ng/mL) [17] were used. Initially, to study the barrier function of the 2D HTM cell monolayers, transendothelial electron resistance (TEER) and FITC-dextran permeability measurements were performed. As shown in Figure 1, upon treatment with a 5 ng/mL solution of $\text{TGF-}\beta$ 2, the TEER values were substantially increased and a decrease in FITC-dextran permeability was observed, and these $\text{TGF-}\beta$ 2 induced changes were significantly suppressed by $\text{PGF2}\alpha$, but not by OMD. This finding suggests that such suppressive effects toward the barrier function in the $\text{TGF-}\beta$ 2-treated 2D HTM monolayers are exclusively FP2 dependent.

We next examined the drug-induced effects of $\text{PGF2}\alpha$ and OMD on $\text{TGF-}\beta$ 2-treated 3D HTM spheroids with respect to their physical properties, size, and stiffness. As shown in Figure 2, the sizes of the $\text{TGF-}\beta$ 2 untreated control 3D HTM spheroids became substantially decreased during the 6-day culture, and these downsizing effects were further enhanced in the case of the $\text{TGF-}\beta$ 2-treated spheroids at days 3 and 6. Furthermore, the $\text{TGF-}\beta$ 2-treated 3D HTM spheroids became significantly larger at day 6 in the presence of either $\text{PGF2}\alpha$ or OMD. Alternatively, the administration of $\text{TGF-}\beta$ 2 significantly induced an increased

stiffness in the 3D HTM spheroids, and the TGF- β 2-induced effect was further increased by the presence of PGF2 α , but not OMD (Figure 3).

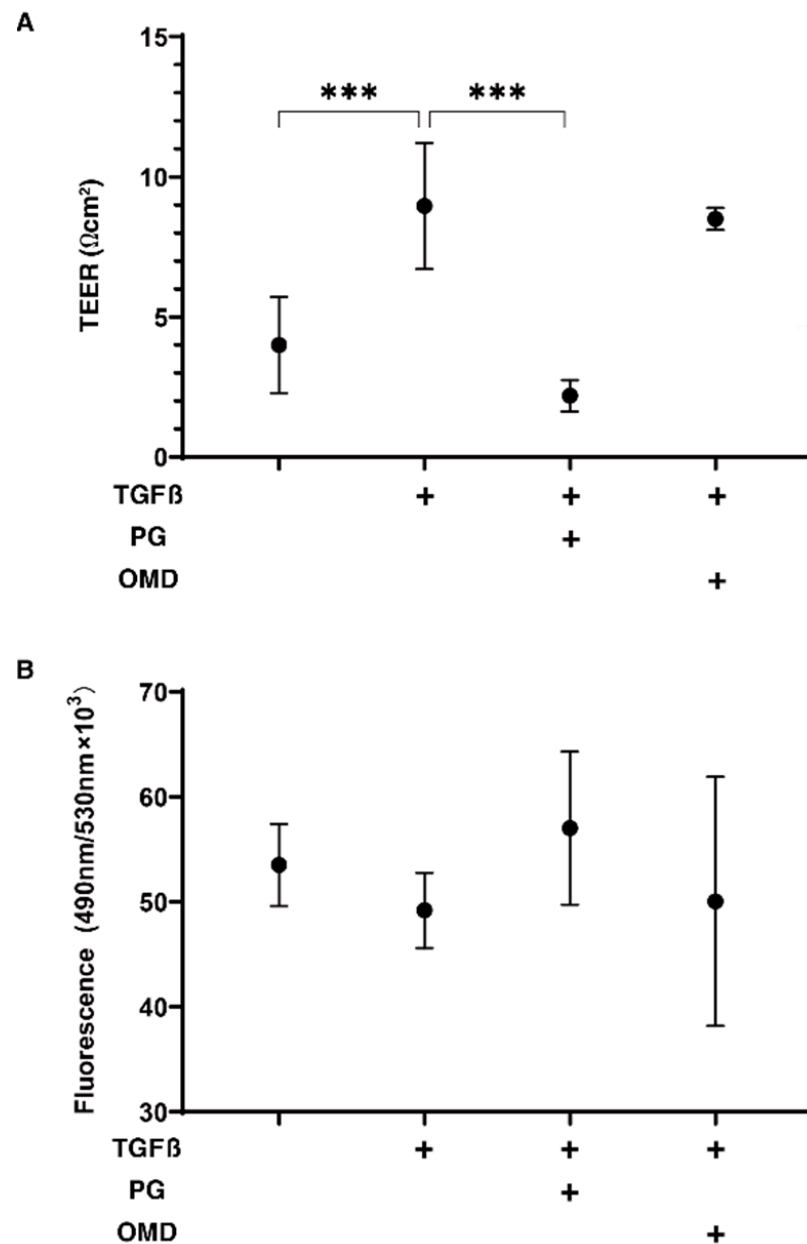


Figure 1. Effects of PGF2 α and the EP2 agonist, omdinenepag (OMD), on barrier functions of TGF β 2-treated 2D HTM monolayers by transendothelial electrical resistance (TEER) (A) and FITC-dextran permeability (B). To compare the effects of 100 nM PGF2 α (PG) and omdinenepag (OMD) on the barrier functions of 5 ng/mL TGF- β 2 (TGF β)-treated 2D HTM monolayers, TEER values (Ωcm^2) and FITC-dextran permeability were measured in addition to the TGF β untreated control, and these values were plotted in panel A and B, respectively. “+” is reagents addition. All experiments were performed using fresh preparations ($n = 3-4$). All data are presented as the arithmetic mean \pm standard error of the mean (SEM). *** $p < 0.005$ (ANOVA followed by a Tukey’s multiple comparison test).

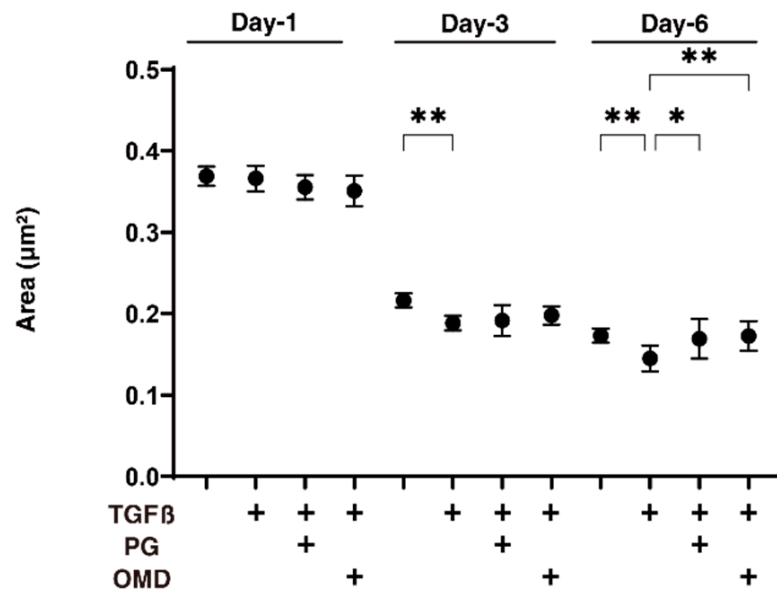


Figure 2. Effects of PGF2α and the EP2 agonist, omidenepag (OMD), on sizes of TGFβ2-treated 3D HTM spheroids at days 1, 3, or 6. To compare the effects of 100 nM PGF2α (PG) and omidenepag (OMD) on the mean sizes of the 5 ng/mL TGF-β2 (TGFβ) HTM 3D spheroids, measurements were made on days 1, 3, or 6 in addition to TGFβ untreated controls, and plotted ($n = 10\text{--}12$ 3D spheroids for each experimental condition). “+” is reagents addition. Data that are presented are the arithmetic mean \pm standard error of the mean (SEM), and statistical differences were determined by ANOVA followed by a Tukey’s multiple comparison test. * $p < 0.05$, ** $p < 0.01$.

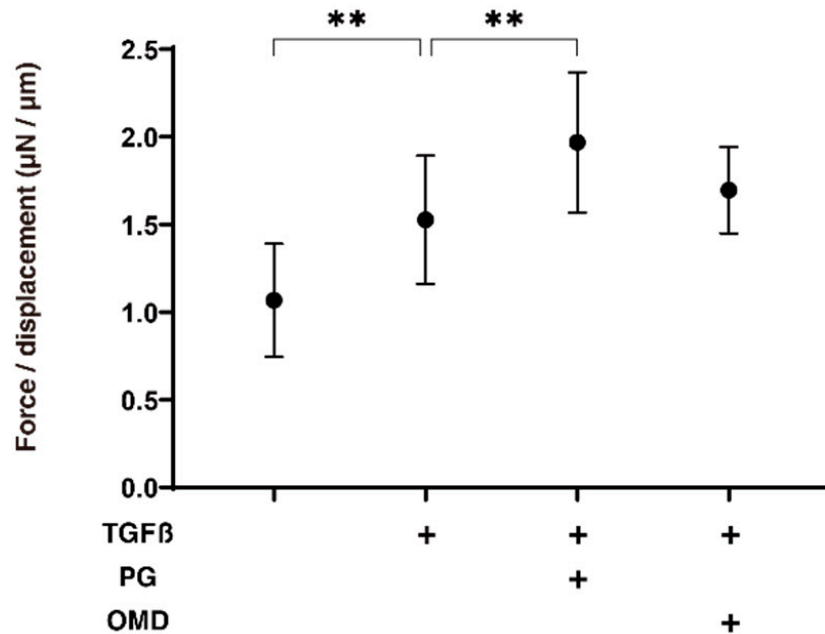


Figure 3. Effects of PGF2α and the EP2 agonist, omidenepag (OMD), on stiffness of TGFβ2-treated 3D HTM spheroids. To compare the effects of 100 nM PGF2α (PG) and omidenepag (OMD) on the stiffness of the 5 ng/mL TGF-β2 (TGFβ) HTM 3D spheroids, those at day 6 were subjected to a micro-squeezer analysis in addition to TGFβ untreated controls. The required force (μN) was measured and force/displacement (μN/μm) were plotted ($n = 10\text{--}12$ 3D spheroids in each experimental condition). “+” is reagents addition. Data presented are the arithmetic mean \pm standard error of the mean (SEM), and statistical differences were determined by ANOVA followed by a Tukey’s multiple comparison test. ** $p < 0.01$.

To elucidate the underlying mechanisms responsible for the above effects by $\text{PGF2}\alpha$ and OMD on the TGF- β 2-treated 2D- and 3D-cultured HTM cells, the expression of ECM proteins (*COL1*, 4, and 6, *FN*, and α *SMA*) was estimated by qPCR analysis and immunolabeling. The administration of TGF- β 2 induced a significant up-regulation in the mRNA expressions of all ECMs molecules (2D), and *COL1*, *COL6*, and *FN* (3D). The addition of $\text{PGF2}\alpha$ or OMD induced a significant up-regulation in *COL4* (2D) and a down-regulation in *COL1* (3D), *COL6* (3D), *FN* (3D), and α *SMA* (3D), and a substantial up-regulation of *COL4* (2D) and down-regulation of *COL6* (3D) and *FN* (3D), respectively (Figure 4). Immunolabeling of 2D-cultured HTM cells with specific antibodies was nearly identical to those for gene expression (Supplemental Figure S1). However, in contrast, the immunolabeling results of the 3D spheroids indicated that the expression of *COL6* was relatively up-regulated and significantly down-regulated by $\text{PGF2}\alpha$ or OMD similarly to mRNA expression (Figure 5). The expressions of the other ECM molecules were not significantly modulated among the 3D HTM spheroid experimental groups (Supplemental Figure S2). In terms of these discrepancies between qPCR and immunolabeling of the 3D spheroids, this was also recognized in our previous study using HTM cells [17,24] as well as other sources of cells [25–27]. As a possible reason for this, we speculate that immunolabeling may adequately reflect the expression of the target molecules that are located on the surface of the 3D spheroids, in contrast to their total expressions detected by qPCR analysis.

To examine this issue further, qPCR analyses of tight junction (TJ)-related proteins in TM, claudin11 (*Cldn11*) and *ZO1* [28,29], ECM regulatory factors; *TIMP1-4*, *MMP2*, 9 and 14, and *CTGF*, and ER stress-related factors; the glucose regulator protein (*GRP*)78, *GRP94*, the X-box binding protein-1 (*XBP1*), spliced *XBP1* (*sXBP1*) and the CCAAT/enhancer-binding protein homologous protein (*CHOP*) were performed. TJ-related molecules and the mRNA expression of *Cldn11* and *ZO1* were significantly up-regulated (2D) or down-regulated (3D) by the presence of $\text{PGF2}\alpha$ or OMD although the values were not affected by TGF- β 2 (Figure 6). While in contrast, *TIMP2* (2D), *TIMP3* and 4 (3D), *MMP2*, 9 and *MMP14* (2D and 3D), *CTGF* (2D and 3D), and all five ER stress-related genes except *GRP78* (2D) or *GRP94*, *XBP*, and *sXBP* (3D) were significantly up-regulated or down-regulated, respectively, upon the administration of a 5 ng/mL solution of TGF- β 2 (Supplemental Figures S3–S5). The addition of $\text{PGF2}\alpha$ or OMD induced a significant down-regulation of *TIMP1* (2D and 3D), *TIMP3* (3D), *MMP14* (3D), *GRP 78* (2D), *GRP 94* (2D), *XBP* (2D), *sXBP* (2D), and *CHOP* (2D and 3D) and an up-regulation of *CTGF* (2D) and a down-regulation of *TIMP3* (3D) as well as all five ER stress-related genes (2D), and an up-regulation of *CTGF* (2D), respectively (Supplemental Figures S3–S5). The above observations are summarized in Table 1; (1) TGF- β 2 induced a significant up-regulation of most of the ECM proteins, ECM regulatory factors, TIMPs and MMPs, and *CTGF* in both 2D- and 3D-cultured HTM cells, but the expression of ER stress-related was different between the 2D- (up-regulated) and the 3D (down-regulated)-cultured HTM cells, and (2) $\text{PGF2}\alpha$ and OMD had similar effects on the expressions of *COL4* (2D), *COL6* and *FN* (3D), TJ-related molecules (2D; up-regulation, 3D; down-regulation), *TIMP3* (3D; up-regulation), *CTGF* (2D; up-regulation) and most of the ER stress-related factors, but some gene expressions including for *COL1* and α *SMA* (3D), *TIMP1* (2D and 3D), *MMP9* (3D), and *CHOP* (3D) were different between two drugs. Therefore, these collective findings suggest that the $\text{PGF2}\alpha$ and OMD induced the up-regulation of TJ-related molecules (2D) and their diverse effects on the expression of several genes may cause diverse effects toward the barrier functions of the 2D HTM monolayers as well as the physical properties of the 3D HTM spheroids, as described above.

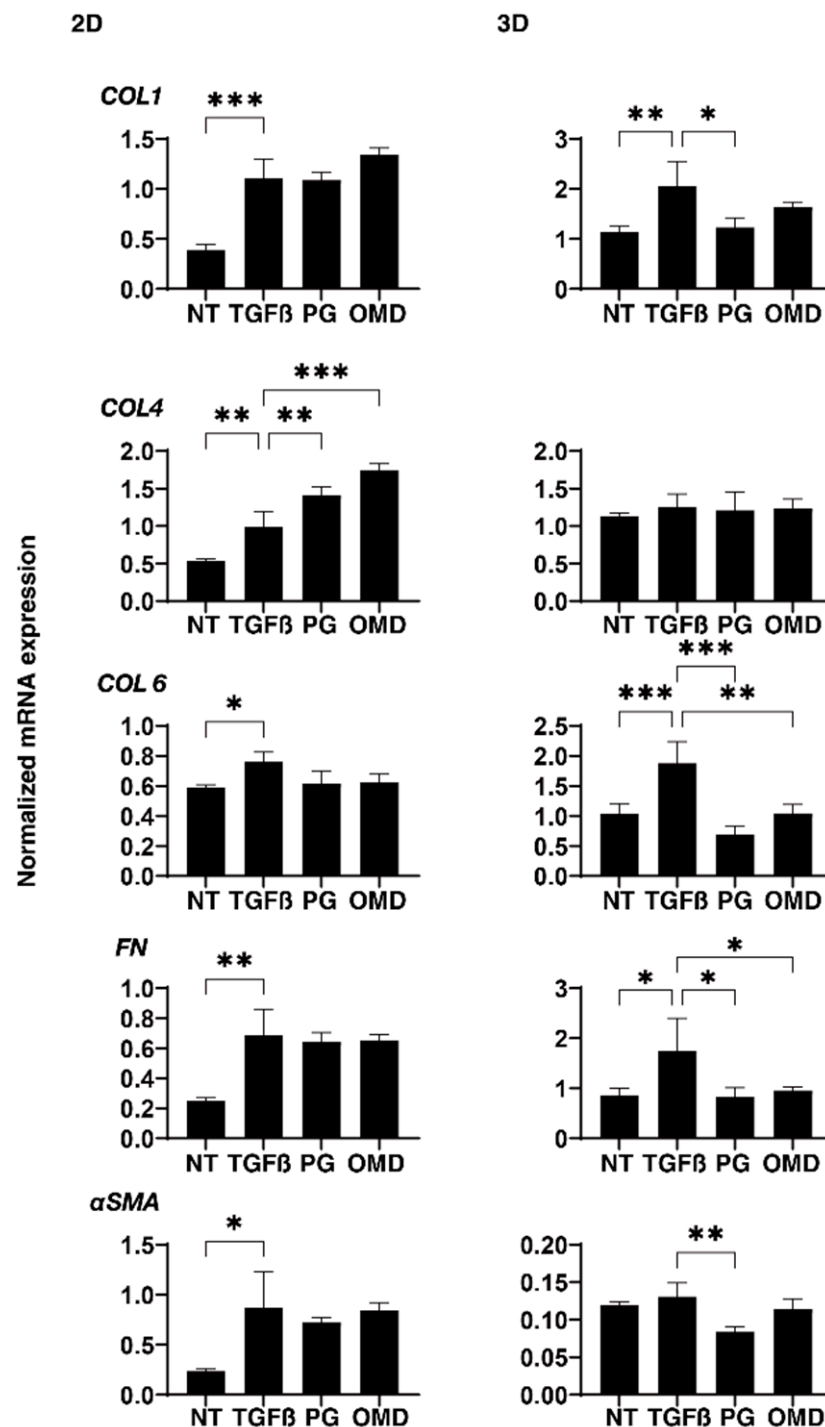


Figure 4. Effects of PGF2α and the EP2 agonist, omidenepag (OMD), on the mRNA expression of ECM proteins in 2D- and 3D-cultured HTM cells. At Day 6, HTM 2D cells and 3D spheroids (NT: non-treated control) and those treated with a 5 ng/mL solution of TGF-β2 (TGFβ) in the absence and presence of 100 nM PGF2α (PG) or the EP2 agonist, omidenepag (OMD) were subjected to qPCR analysis to estimate the expression of mRNA in ECMs (COL1, COL4, COL6, FN and αSMA). Analyses were performed in triplicate using fresh preparations ($n = 12-15$ 3D spheroids each). “+” is reagents addition. Data presented are the arithmetic mean \pm standard error of the mean (SEM), and statistical differences were determined by ANOVA followed by a Tukey’s multiple comparison test. * $p < 0.05$, ** $p < 0.01$, *** $p < 0.005$.

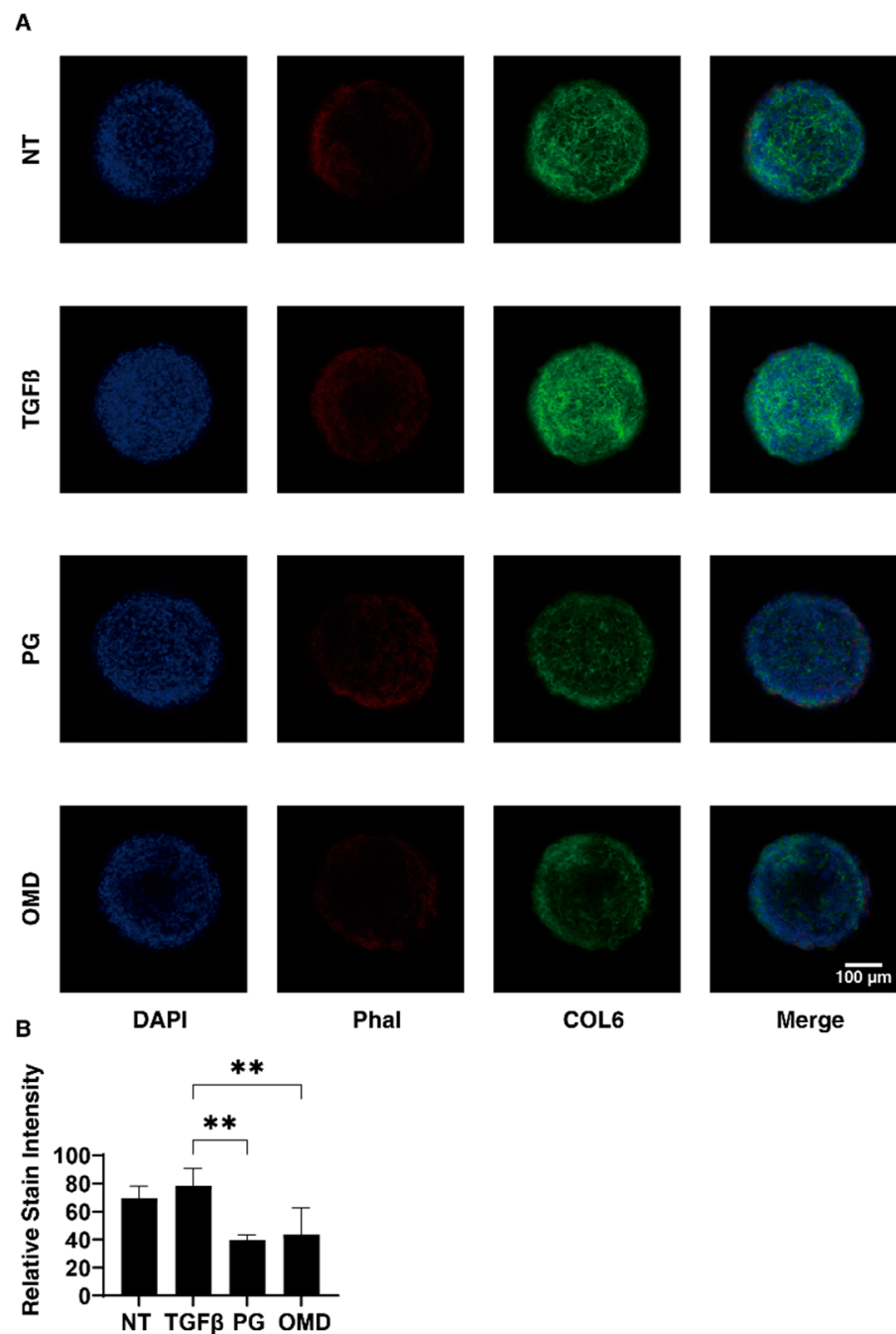


Figure 5. Immunofluorescence images of the expressed COL6 in 3D HTM spheroids. At Day 6, 3D spheroids (NT: non-treated control) and those treated with a 5 ng/mL solution of TGF- β 2 (TGF β) in the absence and presence of 100 nM PGF2 α (PG) or the EP2 agonist, omidenepag (OMD) were immunostained with specific antibodies against COL6 (green), DAPI (blue) and phalloidin (Phal, red). Representative immunolabeling by anti-COL6 are shown in panel (A) (Scale bar: 100 μ m) and the intensities of staining are plotted in panel (B). All experiments were performed in duplicate using fresh preparations consisting of 10 spheroids each. Data presented (total $n = 20$ different 3D spheroids' images) are the arithmetic mean \pm standard error of the mean (SEM), and statistical differences were determined by ANOVA followed by a Tukey's multiple comparison test. ** $p < 0.01$.

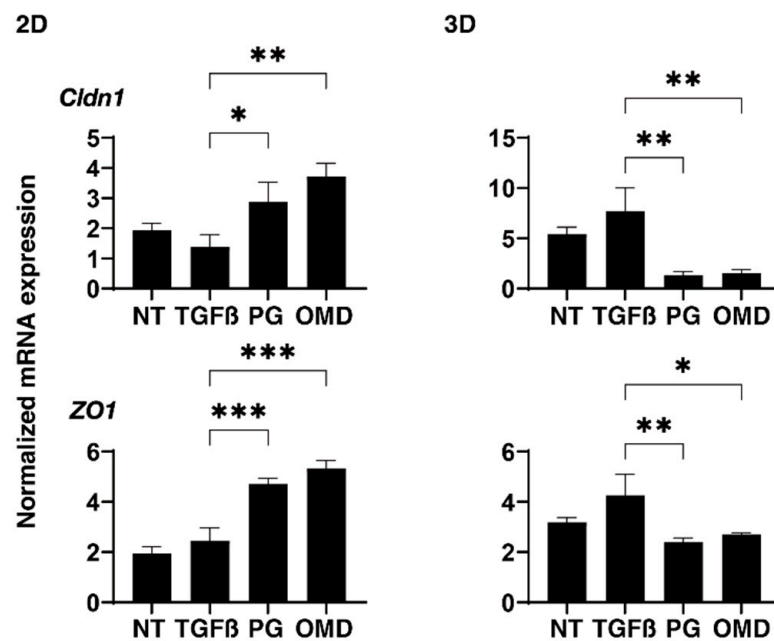


Figure 6. Effects of PGF2α and the EP2 agonist, omidenepag (OMD), on the mRNA expressions of tight junction related proteins in 2D- and 3D-cultured HTM cells. At Day 6, 2D and 3D cultured HTM cells (NT: non-treated control) and those treated with a 5 ng/mL solution of TGF-β2 (TGFβ) in the absence and presence of 100 nM PGF2α (PG) or the EP2 agonist, omidenepag (OMD) were subjected to mRNA expression analysis of mRNA in claudin11 (Cldn11) and ZO1. Analyses were performed in triplicate using fresh preparations (n = 12–15 3D spheroids each). Data presented are the arithmetic mean ± standard error of the mean (SEM), and statistical differences were determined by ANOVA followed by a Tukey’s multiple comparison test. * p < 0.05, ** p < 0.01, *** p < 0.005.

Table 1. Summary of mRNA expressions of ECM proteins, tight junction-related molecules, TIMPs, MMPs, CRGF, and ER stress-related factors.

	2D			3D		
	TGF	PG	OMD	TGF	PG	OMD
COL1	↑↑			↑↑	↓	
COL4	↑↑	↓↓	↓↓			
COL6	↑			↑↑	↓↓	↓
FN	↑↑			↑	↓	↓
αSMA	↑				↓↓	
Cldn11		↑	↑↑		↓↓	↓↓
ZO1		↑↑	↑↑		↓↓	↓
TIMP 1		↓			↓↓	
TIMP 2	↑					
TIMP 3				↑↑	↓↓	↓↓
TIMP 4				↑		
MMP 2	↑			↑↑		
MMP 9	↑			↑↑	↓	
MMP 14	↑			↑↑		
CTGF	↑↑	↑	↑	↑		
GRP 78		↓	↓↓			
GRP 94	↑↑	↓↓	↓↓	↓↓		
XBP	↑↑	↓↓	↓↓	↓		
sXBP	↑↑	↓↓	↓↓	↓↓		
CHOP	↑↑	↓↓	↓↓		↓	

Statistically significant differences between TGF untreated control and TGF, or TGF and PG or OMD are designated as follows; ↑: significant increase (p < 0.05), ↑↑: significant increase (p < 0.01), ↓: significant decrease (p < 0.05), ↓↓: significant decrease (p < 0.01).

At day 6, HTM 2D cells and 3D spheroids (NT: non-treated control) and those treated with a 5 ng/mL solution of TGF- β 2 (TGF β) in the absence and presence of 100 nM PGF2 α (PG) or the EP2 agonist, omidenepag (OMD), were subjected to qPCR analysis to estimate the expression of mRNA in ECMs (*COL1*, *COL4*, *COL6*, *FN*, and *α SMA*). Analyses were performed in triplicate using fresh preparations ($n = 12$ – 15 3D spheroids each). Data presented are the arithmetic mean \pm standard error of the mean (SEM), and statistical differences were determined by ANOVA followed by a Tukey's multiple comparison test. * $p < 0.05$, ** $p < 0.01$, *** $p < 0.005$.

At day 6, 3D spheroids (NT: non-treated control) and those treated with a 5 ng/mL solution of TGF- β 2 (TGF β) in the absence and presence of 100 nM PGF2 α (PG) or the EP2 agonist, omidenepag (OMD), were immunostained with specific antibodies against COL6 (green), DAPI (blue), and phalloidin (Phal, red). Representative immunolabeling by anti-COL6 is shown in panel A (Scale bar: 100 μ m) and the intensities of staining are plotted in panel B. All experiments were performed in duplicate using fresh preparations consisting of 10 spheroids each. Data presented (total $n = 20$ different 3D spheroids' images) are the arithmetic mean \pm standard error of the mean (SEM), and statistical differences were determined by ANOVA followed by a Tukey's multiple comparison test. ** $p < 0.01$.

At day 6, 2D- and 3D-cultured HTM cells (NT: non-treated control) and those treated with a 5 ng/mL solution of TGF- β 2 (TGF β) in the absence and presence of 100 nM PGF2 α (PG) or the EP2 agonist, omidenepag (OMD), were subjected to mRNA expression analysis of mRNA in *claudin11* (*Cldn11*) and *ZO1*. Analyses were performed in triplicate using fresh preparations ($n = 12$ – 15 3D spheroids each). Data presented are the arithmetic mean \pm standard error of the mean (SEM), and statistical differences were determined by ANOVA followed by a Tukey's multiple comparison test. * $p < 0.05$, ** $p < 0.01$, *** $p < 0.005$.

4. Discussion

As compared to conventional 2D cell cultures, 3D spheroid cell cultures have recently received considerable attention for use as suitable in vitro disease models including glaucoma using HTM cells [18,30–32]. However, there may also be some drawbacks to the use of these 3D culture techniques in terms of mimicking the physiological and pathological conditions of human TM due to the presence of unnecessary scaffolds or a collagen matrix. To avoid such potential problems, we recently developed a 3D cell drop culture method as an in vitro model for Graves' orbitopathy [23], deepening upper eyelid sulcus (DUES) [25,27]. In our earlier pilot study, we also applied this method to replicate glaucomatous TM and found that TGF- β 2 significantly induced the downsizing and stiffness of 3D HTM spheroids and that these effects were substantially inhibited by pan-ROCK inhibitors [17]. It is noteworthy that in the current study, we also observed several differences between TGF- β 2-treated 2D and 3D HTM cells in terms of the mRNA expression of ECM molecules and their regulatory factors. As of this writing, our knowledge regarding the molecular mechanisms responsible for causing such diversities between 2D and 3D cells is very limited, despite the fact that the same cells are used. However, quite interestingly, the changes in the gene expressions of the ER stress-related factors tested were observed to be much less in the case of 3D HTM spheroids as compared with 2D HTM cells upon administering a 5 ng/mL solution of TGF- β 2 (Supplemental Figure S5). Therefore, these collective findings suggest that 3D spheroids may be a more stable environment as compared to the corresponding 2D cell cultures of HTM cells. In fact, taking advantage of the use of 3D spheroid cultures, we also reported that this method may be suitable for the screening of several anti-glaucoma drugs toward TGF- β 2 and dexamethasone-treated 3D HTM spheroids as in vitro models for HTM with primary open-angle glaucoma and steroid-induced glaucoma [20,21,24].

In terms of the possible hypotensive effects of both the PGF2 α -ags and EP2 agonists, it has been suggested that an increased uveoscleral outflow pathway through the activation of matrix metalloproteinases (MMP) and ECM remodeling is primarily involved [33–37]. However, it has also been suggested that both drugs may also affect the conventional

TM outflow, the main route for AH drainage based on the presence of both FP and EP2 receptors on TM tissues [38–41]. FP and EP2 receptors are functionally characterized as contractile and relaxant receptors that are responsible for the contraction of smooth muscle cells [42–46] as well as Schlemm’s canal endothelial cells [46,47]. While, in contrast, it was reported that FP receptors mediated an enhancement in pulmonary and myocardial fibrosis [48,49], despite the fact that lung fibrosis had deteriorated upon the deletion of the EP2 receptor [50]. These collective observations suggest that the stimulation and inhibition of FP or EP2 receptors may modulate the structure and function of the TM in different ways. In the current study, we also found that the PGF2 α and the EP2 agonist, OMD, had different effects on the barrier functions by TEER and FITC-dextran permeability analyses of the 2D HTM monolayers and the physical property analyses of the TGF β 2-induced 3D HTM spheroids. That is, as shown in Table 2, PGF2 α induced a decrease in the TEER values of 2D HTM monolayers and an increase in the stiffness of the 3D HTM spheroids, but OMD had no effect on these parameters, although both PGF2 α and OMD caused an increase in the size of the 3D HTM spheroids. Interestingly, the pan-ROCK inhibitors, ripasudil (Rip) also induced similar changes in the TEER values and 3D spheroid size but caused quite different effects on 3D spheroid stiffness as compared to PGF2 α and OMD.

Table 2. Comparison of the drug-induced effects on the TEER values of the 2D HTM monolayers, and physical properties, size and stiffness, and mRNA expression of ECM molecules with 3D HTM spheroids.

	PGF2 α	OMD	Rip*
2D monolayer			
TEER	↓	(–)	↓
3D spheroid			
size	↑	↑	↑
stiffness	↑	(–)	↓
ECM expression			
2D	COL4 ↑	COL4 ↑	(N.D.)
3D			COL1 ↓ COL4 ↓
	COL6 ↓ FN ↓ α SMA ↓	COL6 ↓ FN ↓	

PGF2 α ; prostaglandin F2 α , OMD; omidenepag, Rip; ripasudil, TEER; Transendothelial electron resistance, COL1; collagen 1, COL4; collagen 4, COL6; collagen 6, FN; fibronectin, α SMA; α smooth muscle actin, ↑: significant increase, ↓: significant decrease, (–): not significant change. N.D.; not determined. Data related to Rip* were recruited from our previous study [17].

In terms of the fibrotic changes of TM cells, TGF- β 2 activates cytoplasmic Smad2/3 leading to the up-regulation of the expression of various ECM molecules, such as FN and COL4, which induced an impediment to AH outflow through the TM, ultimately resulting in an elevation in IOP levels [51]. It was revealed that both the FP agonist, latanoprost, and the EP2 agonist, butaprost, inhibited TGF- β 2-mediated collagen deposition [18]. In fact, a loss of collagen materials within the TM was also observed upon the treatment of cynomolgus monkeys with either latanoprost [34] or butaprost [33] for a period of one year. In addition, another FP agonist, fluprostenol, was reported to induce a decrease in the expression of COL4 and 6 that was induced by CTGF in cultured TM cells [52]. In the current study, we also found that TGF- β 2 caused a significant up-regulation of the most of ECMs tested and that PGF2 α or OMD induced a significant up-regulation of network-forming COL4 [53] and the down-regulation of beaded-filament-forming COL6 [53], FN, and α SMA. If 3D spheroid size and stiffness were mainly related with network-forming COL4 and fibril forming COL1, then the PG- or OMD-induced down-regulation of COL6, FN, and α SMA would result in a relative increase in COL1 content, which provides a possible explanation for why PG or OMD caused changes in both the size and stiffness of the 3D spheroids.

The findings presented in this study indicate that PGF2 α and OMD significantly and differently modulated the TEER values and FITC-dextran permeability of TGF- β 2-treated 2D HTM monolayers in addition to the physical properties of the TGF- β 2-treated 3D HTM spheroids, as described above. It is well known that these barrier functions appear to exclusively depend on TJ properties [28,29]. In fact, in our current study, we also observed that PGF2 α and OMD induced a significant up-regulation of Cldn11 and ZO1 in the 2D HTM monolayers, although no significant difference was observed between them despite the significant diverse effects toward TEER values (Figure 6). Therefore, these collective findings suggest that additional unknown mechanisms may well be involved, and the following study limitations that need to be discussed are as follows; (1) rationale mechanisms for causing diversity in the permeability of the 2D NTM monolayer between PGF2 α and OMD which have not been fully elucidated, and (2) the relationship between such collective observations and the ease of aqueous outflow of the human TM for a better understanding of the roles of FP or EP2 agonists in the AH dynamics of HTM. Therefore, further investigation will be required to obtain additional insights into the molecular mechanisms causing diverse effects by PGF2 α and OMD for future therapeutic strategies for the treatment of glaucoma using PGF2 α -ags and EP2 agonist.

Supplementary Materials: The following supporting information can be downloaded at: <https://www.mdpi.com/article/10.3390/jcm11061652/s1>. Figure S1. Immunofluorescence images of the expressed ECM proteins in 2D cultured HTM cells. Figure S2. Immunofluorescence images of the expressed ECM proteins including COL1, COL4, FN and α SMA in 3D HTM spheroids. Figure S3. Effects of PGF2 α and the EP2 agonist, omdinenepag (OMD) on the mRNA expression of TIMPs in 2D and 3D cultured HTM cells. Figure S4. Effects of PGF2 α and the EP2 agonist, omdinenepag (OMD) on the mRNA expression of MMPs and CTGF in 2D and 3D cultured HTM cells. Figure S5. Effects of PGF2 α and the EP2 agonist, omdinenepag (OMD) on the mRNA expression of ER stress related factors in 2D and 3D cultured HTM cells. Table S1. A. Sequences of primers used in the qPCR. B. Running protocols for a real time RT-PCR of TaqMan based and SYBR based analyses. Table S2. Product data of 1st antibodies for immunocytochemistry.

Author Contributions: S.S. performed the experiments, analyzed data and wrote the paper; M.F. analyzed data and participated in the writing of the paper; Y.T. performed experiments and analyzed data; A.U. performed experiments and analyzed data; Y.I. analyzed data; F.H. analyzed the data; H.O. designed the experiments and wrote the paper; M.W. performed the experiments, analyzed data and wrote the paper. Both authors (S.S. and M.F.) contributed equally to this manuscript. All authors have read and agreed to the published version of the manuscript.

Funding: This research received no external funding.

Institutional Review Board Statement: Not applicable.

Informed Consent Statement: Not applicable.

Data Availability Statement: The data that support the findings of this study are available from the corresponding author upon reasonable request.

Conflicts of Interest: The authors declare no conflict of interest.

References

1. Quigley, H.A.; Broman, A.T. The number of people with glaucoma worldwide in 2010 and 2020. *Br. J. Ophthalmol.* **2006**, *90*, 262–267. [[CrossRef](#)] [[PubMed](#)]
2. Caprioli, J.; Coleman, A.L. Blood pressure, perfusion pressure, and glaucoma. *Am. J. Ophthalmol.* **2010**, *149*, 704–712. [[CrossRef](#)] [[PubMed](#)]
3. Weinreb, R.N.; Khaw, P.T. Primary open-angle glaucoma. *Lancet* **2004**, *363*, 1711–1720. [[CrossRef](#)]
4. van der Valk, R.; Webers, C.A.; Schouten, J.S.; Zeegers, M.P.; Hendrikse, F.; Prins, M.H. Intraocular pressure-lowering effects of all commonly used glaucoma drugs: A meta-analysis of randomized clinical trials. *Ophthalmology* **2005**, *112*, 1177–1185. [[CrossRef](#)] [[PubMed](#)]
5. Gabelt, B.T.; Gottanka, J.; Lütjen-Drecoll, E.; Kaufman, P.L. Aqueous humor dynamics and trabecular meshwork and anterior ciliary muscle morphologic changes with age in rhesus monkeys. *Investig. Ophthalmol. Vis. Sci.* **2003**, *44*, 2118–2125. [[CrossRef](#)] [[PubMed](#)]

6. Filla, M.S.; Liu, X.; Nguyen, T.D.; Polansky, J.R.; Brandt, C.R.; Kaufman, P.L.; Peters, D.M. In Vitro Localization of TIGR/MYOC in Trabecular Meshwork Extracellular Matrix and Binding to Fibronectin. *Investig. Ophthalmol. Vis. Sci.* **2002**, *43*, 151–161.
7. Kasetti, R.B.; Maddineni, P.; Patel, P.D.; Searby, C.; Sheffield, V.C.; Zode, G.S. Transforming growth factor β 2 (TGF β 2) signaling plays a key role in glucocorticoid-induced ocular hypertension. *J. Biol. Chem.* **2018**, *293*, 9854–9868. [[CrossRef](#)]
8. Yang, Q.; Li, Y.; Luo, L. Effect of Myricetin on Primary Open-angle Glaucoma. *Transl. Neurosci.* **2018**, *9*, 132–141. [[CrossRef](#)]
9. Fuchshofer, R.; Welge-Lüssen, U.; Lütjen-Drecoll, E. The effect of TGF- β 2 on human trabecular meshwork extracellular proteolytic system. *Exp. Eye Res.* **2003**, *77*, 757–765. [[CrossRef](#)]
10. European Glaucoma Society. Terminology and Guidelines for Glaucoma, 4th Edition—Chapter 3: Treatment principles and options Supported by the EGS Foundation: Part 1: Foreword; Introduction; Glossary; Chapter 3 Treatment principles and options. *Br. J. Ophthalmol.* **2017**, *101*, 130–195. [[CrossRef](#)]
11. Alm, A. Latanoprost in the treatment of glaucoma. *Clin. Ophthalmol.* **2014**, *8*, 1967–1985. [[PubMed](#)]
12. Ota, T.; Aihara, M.; Narumiya, S.; Araie, M. The effects of prostaglandin analogues on IOP in prostanoid FP-receptor-deficient mice. *Investig. Ophthalmol. Vis. Sci.* **2005**, *46*, 4159–4163. [[CrossRef](#)] [[PubMed](#)]
13. Aihara, M.; Lu, F.; Kawata, H.; Tanaka, Y.; Yamamura, K.; Odani-Kawabata, N.; Shams, N.K. Pharmacokinetics, Safety, and Intraocular Pressure-Lowering Profile of Omidenepag Isopropyl, a Selective, Nonprostaglandin, Prostanoid EP2 Receptor Agonist, in Healthy Japanese and Caucasian Volunteers (Phase I Study). *J. Ocul. Pharmacol. Ther.* **2019**, *35*, 542–550. [[CrossRef](#)] [[PubMed](#)]
14. Aihara, M.; Lu, F.; Kawata, H.; Iwata, A.; Odani-Kawabata, N.; Shams, N.K. Omidenepag Isopropyl Versus Latanoprost in Primary Open-Angle Glaucoma and Ocular Hypertension: The Phase 3 AYAME Study. *Am. J. Ophthalmol.* **2020**, *220*, 53–63. [[CrossRef](#)] [[PubMed](#)]
15. Impagnatiello, F.; Bastia, E.; Almirante, N.; Brambilla, S.; Duquesroix, B.; Kothe, A.C.; Bergamini, M.V.W. Prostaglandin analogues and nitric oxide contribution in the treatment of ocular hypertension and glaucoma. *Br. J. Pharmacol.* **2019**, *176*, 1079–1089. [[CrossRef](#)]
16. Fuwa, M.; Toris, C.B.; Fan, S.; Taniguchi, T.; Ichikawa, M.; Odani-Kawabata, N.; Iwamura, R.; Yoneda, K.; Matsugi, T.; Shams, N.K.; et al. Effects of a Novel Selective EP2 Receptor Agonist, Omidenepag Isopropyl, on Aqueous Humor Dynamics in Laser-Induced Ocular Hypertensive Monkeys. *J. Ocul. Pharmacol. Ther.* **2018**, *34*, 531–537. [[CrossRef](#)]
17. Ota, C.; Ida, Y.; Ohguro, H.; Hikage, F. ROCK inhibitors beneficially alter the spatial configuration of TGF β 2-treated 3D organoids from a human trabecular meshwork (HTM). *Sci. Rep.* **2020**, *10*, 20292. [[CrossRef](#)]
18. Kalouche, G.; Beguier, F.; Bakria, M.; Melik-Parsadaniantz, S.; Leriche, C.; Debeir, T.; Rostène, W.; Baudouin, C.; Vigé, X. Activation of Prostaglandin FP and EP2 Receptors Differently Modulates Myofibroblast Transition in a Model of Adult Primary Human Trabecular Meshwork Cells. *Investig. Ophthalmol. Vis. Sci.* **2016**, *57*, 1816–1825. [[CrossRef](#)]
19. Keller, K.E.; Bhattacharya, S.K.; Borrás, T.; Brunner, T.M.; Chansangpetch, S.; Clark, A.F.; Dismuke, W.M.; Du, Y.; Elliott, M.H.; Ethier, C.R.; et al. Consensus recommendations for trabecular meshwork cell isolation, characterization and culture. *Exp. Eye Res.* **2018**, *171*, 164–173. [[CrossRef](#)]
20. Watanabe, M.; Ida, Y.; Ohguro, H.; Ota, C.; Hikage, F. Diverse effects of pan-ROCK and ROCK2 inhibitors on 2D and 3D cultured human trabecular meshwork (HTM) cells treated with TGF β 2. *Sci. Rep.* **2021**, *11*, 15286. [[CrossRef](#)]
21. Watanabe, M.; Ida, Y.; Furuhashi, M.; Tsugeno, Y.; Ohguro, H.; Hikage, F. Screening of the Drug-Induced Effects of Prostaglandin EP2 and FP Agonists on 3D Cultures of Dexamethasone-Treated Human Trabecular Meshwork Cells. *Biomedicines* **2021**, *9*, 930. [[CrossRef](#)] [[PubMed](#)]
22. Kaneko, Y.; Ohta, M.; Inoue, T.; Mizuno, K.; Isobe, T.; Tanabe, S.; Tanihara, H. Effects of K-115 (Ripasudil), a novel ROCK inhibitor, on trabecular meshwork and Schlemm’s canal endothelial cells. *Sci. Rep.* **2016**, *6*, 19640. [[CrossRef](#)] [[PubMed](#)]
23. Hikage, F.; Atkins, S.; Kahana, A.; Smith, T.J.; Chun, T.H. HIF2A-LOX Pathway Promotes Fibrotic Tissue Remodeling in Thyroid-Associated Orbitopathy. *Endocrinology* **2019**, *160*, 20–35. [[CrossRef](#)] [[PubMed](#)]
24. Watanabe, M.; Ida, Y.; Ohguro, H.; Ota, C.; Hikage, F. Establishment of appropriate glaucoma models using dexamethasone or TGF β 2 treated three-dimension (3D) cultured human trabecular meshwork (HTM) cells. *Sci. Rep.* **2021**, *11*, 19369. [[CrossRef](#)] [[PubMed](#)]
25. Itoh, K.; Hikage, F.; Ida, Y.; Ohguro, H. Prostaglandin F 2α Agonists Negatively Modulate the Size of 3D Organoids from Primary Human Orbital Fibroblasts. *Investig. Ophthalmol. Vis. Sci.* **2020**, *61*, 13. [[CrossRef](#)]
26. Itoh, K.; Ida, Y.; Ohguro, H.; Hikage, F. Prostaglandin F 2α agonists induced enhancement in collagen1 expression is involved in the pathogenesis of the deepening of upper eyelid sulcus. *Sci. Rep.* **2021**, *11*, 9002. [[CrossRef](#)]
27. Ida, Y.; Hikage, F.; Itoh, K.; Ida, H.; Ohguro, H. Prostaglandin F 2α agonist-induced suppression of 3T3-L1 cell adipogenesis affects spatial formation of extra-cellular matrix. *Sci. Rep.* **2020**, *10*, 7958. [[CrossRef](#)]
28. Li, X.; Acott, T.S.; Nagy, J.I.; Kelley, M.J. ZO-1 associates with α 3 integrin and connexin43 in trabecular meshwork and Schlemm’s canal cells. *Int. J. Physiol. Pathophysiol. Pharmacol.* **2020**, *12*, 1–10.
29. Tam, L.C.; Reina-Torres, E.; Sherwood, J.M.; Cassidy, P.S.; Crosbie, D.E.; Lütjen-Drecoll, E.; Flügel-Koch, C.; Perkumas, K.; Humphries, M.M.; Kiang, A.S.; et al. Enhancement of Outflow Facility in the Murine Eye by Targeting Selected Tight-Junctions of Schlemm’s Canal Endothelia. *Sci. Rep.* **2017**, *7*, 40717. [[CrossRef](#)]
30. Torrejon, K.Y.; Papke, E.L.; Halman, J.R.; Bergkvist, M.; Danias, J.; Sharfstein, S.T.; Xie, Y. TGF β 2-induced outflow alterations in a bioengineered trabecular meshwork are offset by a rho-associated kinase inhibitor. *Sci. Rep.* **2016**, *6*, 38319. [[CrossRef](#)]

31. Huh, D.; Hamilton, G.A.; Ingber, D.E. From 3D cell culture to organs-on-chips. *Trends Cell Biol.* **2011**, *21*, 745–754. [[CrossRef](#)] [[PubMed](#)]
32. Vernazza, S.; Tirendi, S.; Scarfi, S.; Passalacqua, M.; Oddone, F.; Traverso, C.E.; Rizzato, I.; Bassi, A.M.; Saccà, S.C. 2D- and 3D-cultures of human trabecular meshwork cells: A preliminary assessment of an in vitro model for glaucoma study. *PLoS ONE* **2019**, *14*, e0221942. [[CrossRef](#)]
33. Nilsson, S.F.; Drecoll, E.; Lütjen-Drecoll, E.; Toris, C.B.; Krauss, A.H.; Kharlamb, A.; Nieves, A.; Guerra, T.; Woodward, D.F. The prostanoid EP2 receptor agonist butaprost increases uveoscleral outflow in the cynomolgus monkey. *Investig. Ophthalmol. Vis. Sci.* **2006**, *47*, 4042–4049. [[CrossRef](#)] [[PubMed](#)]
34. Richter, M.; Krauss, A.H.; Woodward, D.F.; Lütjen-Drecoll, E. Morphological changes in the anterior eye segment after long-term treatment with different receptor selective prostaglandin agonists and a prostamide. *Investig. Ophthalmol. Vis. Sci.* **2003**, *44*, 4419–4426. [[CrossRef](#)] [[PubMed](#)]
35. el-Shabrawi, Y.; Eckhardt, M.; Berghold, A.; Faulborn, J.; Auboeck, L.; Mangge, H.; Ardjomand, N. Synthesis pattern of matrix metalloproteinases (MMPs) and inhibitors (TIMPs) in human explant organ cultures after treatment with latanoprost and dexamethasone. *Eye* **2000**, *14 Pt 3A*, 375–383. [[CrossRef](#)] [[PubMed](#)]
36. Gatton, D.D.; Sagara, T.; Lindsey, J.D.; Gabelt, B.T.; Kaufman, P.L.; Weinreb, R.N. Increased matrix metalloproteinases 1, 2, and 3 in the monkey uveoscleral outflow pathway after topical prostaglandin F(2 alpha)-isopropyl ester treatment. *Arch. Ophthalmol.* **2001**, *119*, 1165–1170. [[CrossRef](#)] [[PubMed](#)]
37. Weinreb, R.N.; Lindsey, J.D.; Marchenko, G.; Marchenko, N.; Angert, M.; Strongin, A. Prostaglandin FP agonists alter metalloproteinase gene expression in sclera. *Investig. Ophthalmol. Vis. Sci.* **2004**, *45*, 4368–4377. [[CrossRef](#)]
38. Lim, K.S.; Nau, C.B.; O’Byrne, M.M.; Hodge, D.O.; Toris, C.B.; McLaren, J.W.; Johnson, D.H. Mechanism of action of bimatoprost, latanoprost, and travoprost in healthy subjects. A crossover study. *Ophthalmology* **2008**, *115*, 790–795.e4. [[CrossRef](#)]
39. Toris, C.B.; Gabelt, B.T.; Kaufman, P.L. Update on the mechanism of action of topical prostaglandins for intraocular pressure reduction. *Surv. Ophthalmol.* **2008**, *53* (Suppl. 1), S107–S120. [[CrossRef](#)]
40. Schlötzer-Schrehardt, U.; Zenkel, M.; Nüsing, R.M. Expression and localization of FP and EP prostanoid receptor subtypes in human ocular tissues. *Investig. Ophthalmol. Vis. Sci.* **2002**, *43*, 1475–1487.
41. Biswas, S.; Bhattacharjee, P.; Paterson, C.A. Prostaglandin E2 receptor subtypes, EP1, EP2, EP3 and EP4 in human and mouse ocular tissues—A comparative immunohistochemical study. *Prostaglandins Leukot. Essent. Fat. Acids* **2004**, *71*, 277–288. [[CrossRef](#)] [[PubMed](#)]
42. Hirata, T.; Narumiya, S. Prostanoid receptors. *Chem. Rev.* **2011**, *111*, 6209–6230. [[CrossRef](#)] [[PubMed](#)]
43. Kaddour-Djebbar, I.; Ansari, H.R.; Akhtar, R.A.; Abdel-Latif, A.A. Species differences in the effects of prostanoids on MAP kinase phosphorylation, myosin light chain phosphorylation and contraction in bovine and cat iris sphincter smooth muscle. *Prostaglandins Leukot. Essent. Fat. Acids* **2005**, *72*, 49–57. [[CrossRef](#)] [[PubMed](#)]
44. Poyer, J.F.; Millar, C.; Kaufman, P.L. Prostaglandin F2 alpha effects on isolated rhesus monkey ciliary muscle. *Investig. Ophthalmol. Vis. Sci.* **1995**, *36*, 2461–2465.
45. Vysniauskiene, I.; Allemann, R.; Flammer, J.; Haefliger, I.O. Vasoactive responses of U46619, PGF2alpha, latanoprost, and travoprost in isolated porcine ciliary arteries. *Investig. Ophthalmol. Vis. Sci.* **2006**, *47*, 295–298. [[CrossRef](#)] [[PubMed](#)]
46. Krauss, A.H.; Wiederholt, M.; Sturm, A.; Woodward, D.F. Prostaglandin effects on the contractility of bovine trabecular meshwork and ciliary muscle. *Exp. Eye Res.* **1997**, *64*, 447–453. [[CrossRef](#)] [[PubMed](#)]
47. Wang, J.W.; Woodward, D.F.; Stamer, W.D. Differential effects of prostaglandin E2-sensitive receptors on contractility of human ocular cells that regulate conventional outflow. *Investig. Ophthalmol. Vis. Sci.* **2013**, *54*, 4782–4790. [[CrossRef](#)]
48. Oga, T.; Matsuoka, T.; Yao, C.; Nonomura, K.; Kitaoka, S.; Sakata, D.; Kita, Y.; Tanizawa, K.; Taguchi, Y.; Chin, K.; et al. Prostaglandin F(2alpha) receptor signaling facilitates bleomycin-induced pulmonary fibrosis independently of transforming growth factor-beta. *Nat. Med.* **2009**, *15*, 1426–1430. [[CrossRef](#)]
49. Ding, W.Y.; Liu, L.; Wang, Z.H.; Tang, M.X.; Ti, Y.; Han, L.; Zhang, L.; Zhang, Y.; Zhong, M.; Zhang, W. FP-receptor gene silencing ameliorates myocardial fibrosis and protects from diabetic cardiomyopathy. *J. Mol. Med.* **2014**, *92*, 629–640. [[CrossRef](#)]
50. Moore, B.B.; Ballinger, M.N.; White, E.S.; Green, M.E.; Herrygers, A.B.; Wilke, C.A.; Toews, G.B.; Peters-Golden, M. Bleomycin-induced E prostanoid receptor changes alter fibroblast responses to prostaglandin E2. *J. Immunol.* **2005**, *174*, 5644–5649. [[CrossRef](#)]
51. Fleenor, D.L.; Shepard, A.R.; Hellberg, P.E.; Jacobson, N.; Pang, I.-H.; Clark, A.F. TGFβ2-Induced Changes in Human Trabecular Meshwork: Implications for Intraocular Pressure. *Investig. Ophthalmol. Vis. Sci.* **2006**, *47*, 226–234. [[CrossRef](#)] [[PubMed](#)]
52. Fuchshofer, R.; Kuespert, S.; Junglas, B.; Tamm, E.R. The prostaglandin f2α analog fluprostenol attenuates the fibrotic effects of connective tissue growth factor on human trabecular meshwork cells. *J. Ocul. Pharmacol. Ther.* **2014**, *30*, 237–245. [[CrossRef](#)] [[PubMed](#)]
53. Onursal, C.; Dick, E.; Angelidis, I.; Schiller, H.B.; Staab-Weijnitz, C.A. Collagen Biosynthesis, Processing, and Maturation in Lung Ageing. *Front. Med.* **2021**, *8*, 593874. [[CrossRef](#)] [[PubMed](#)]